International Journal of Neuropsychopharmacology (2013), **16**, 1361–1371. © CINP 2012
doi:10.1017/S146114571200140X

ARTICLE

Lipid raft integrity affects $GABA_A$ receptor, but not NMDA receptor modulation by psychopharmacological compounds

Caroline Nothdurfter[1,2], Sascha Tanasic[1,2], Barbara Di Benedetto[1,2], Manfred Uhr[2], Eva-Maria Wagner[2], Kate E. Gilling[3], Chris G. Parsons[3], Theo Rein[2], Florian Holsboer[2], Rainer Rupprecht[1,2] and Gerhard Rammes[2,4]

[1] *Department of Psychiatry and Psychotherapy, University Regensburg, Regensburg, Germany*
[2] *Max-Planck-Institute of Psychiatry, Munich, Germany*
[3] *In Vitro Pharmacology, Preclinical Research and Development, Merz Pharmaceuticals GmbH, Frankfurt am Main, Germany*
[4] *Department of Anesthesiology, Technische Universität München, Munich, Germany*

Abstract

Lipid rafts have been shown to play an important role for G-protein mediated signal transduction and the function of ligand-gated ion channels including their modulation by psychopharmacological compounds. In this study, we investigated the functional significance of the membrane distribution of NMDA and $GABA_A$ receptor subunits in relation to the accumulation of the tricyclic antidepressant desipramine (DMI) and the benzodiazepine diazepam (Diaz). In the presence of Triton X-100, which allowed proper separation of the lipid raft marker proteins caveolin-1 and flotillin-1 from the transferrin receptor, all receptor subunits were shifted to the non-raft fractions. In contrast, under detergent-free conditions, NMDA and $GABA_A$ receptor subunits were detected both in raft and non-raft fractions. Diaz was enriched in non-raft fractions without Triton X-100 in contrast to DMI, which preferentially accumulated in lipid rafts. Impairment of lipid raft integrity by methyl-β-cyclodextrine (MβCD)-induced cholesterol depletion did not change the inhibitory effect of DMI at the NMDA receptor, whereas it enhanced the potentiating effect of Diaz at the $GABA_A$ receptor at non-saturating concentrations of GABA. These results support the hypothesis that the interaction of benzodiazepines with the $GABA_A$ receptor likely occurs outside of lipid rafts while the antidepressant DMI acts on ionotropic receptors both within and outside these membrane microdomains.

Received 3 September 2012; Reviewed 24 September 2012; Revised 11 October 2012; Accepted 18 October 2012; First published online 10 December 2012

Key words: Antidepressants, benzodiazepines, $GABA_A$ receptor, lipid rafts, NMDA receptor.

Introduction

Lipid rafts are distinct microdomains within the cell membrane which are enriched in cholesterol and glycosphingolipids (Pike, 2004). These heterogeneous and dynamic structures float within the membrane bilayer allowing lipids and proteins to move in and out of these membrane microdomains (Kusumi and Suzuki, 2005). The concept of lipid rafts has attracted considerable interest because these structures may affect membrane trafficking and signal transduction processes (Tsiu-Pierchala et al., 2002; Patel et al., 2008).

There is increasing evidence that lipid raft association can also influence neurotransmitter receptor function by affecting transmitter binding, receptor trafficking and clustering (Allen et al., 2007). In post-mortem brain tissue of patients with major depression, G-protein subunit (Gs)α was more likely associated with lipid rafts, where it turned out to be less likely coupled to adenylyl cyclase (Donati et al., 2008). Moreover, Gsα-mediated signalling was enhanced by chronic treatment with antidepressants, which prevented the accumulation of Gsα in lipid rafts (Donati and Rasenick, 2005). With regard to ligand-gated ion channels, the serotonin $(5\text{-HT})_{3A}$ receptor has been detected in raft-like domains (Eisensamer et al., 2005). Likewise the $GABA_A$ receptor subunit α1 has been reported to be lipid raft associated (Dalskov et al., 2005), whereas a differential distribution of synaptic and extrasynaptic $GABA_A$ receptor subunits has recently been demonstrated (Li et al., 2007). Also the localization of NMDA receptors within the cell membrane appears to depend on the respective subunit composition (Hering et al., 2003; Guirland et al., 2004).

A variety of antidepressants and antipsychotics accumulate in raft-like domains, which exert their functional antagonistic effects at the 5-HT_3 receptor (Eisensamer et al., 2003, 2005; Rammes et al., 2004). More

Author for correspondence: Dr C. Nothdurfter, Department of Psychiatry and Psychotherapy, University Regensburg, Universitätsstrasse 84, 93053 Regensburg, Germany.
Tel.: +49 941 941 2059 *Fax*: +49 941 941 2065
Email: Caroline.Nothdurfter@medbo.de

recently, we showed that 5-HT_3 receptor function depends on lipid raft integrity, whereas the ability of antidepressants to modulate this receptor is retained after lipid raft impairment (Nothdurfter et al., 2010).

So far, no data are available on the significance of lipid rafts for the modulation of NMDA and $GABA_A$ receptors – crucial members of the most abundant excitatory and inhibitory neurotransmitter systems in the central nervous system – by antidepressants and benzodiazepines. We therefore investigated the effect of lipid raft integrity on the allosteric modulation of $GABA_A$ receptor function by diazepam (Diaz) and on the modulation of NMDA receptor function by the tricyclic antidepressant desipramine (DMI). Moreover, the membrane domain distribution of the receptor subunits and compounds was investigated using different conditions of lipid raft isolating procedures.

Method and materials

Chemicals and drugs

For stock solutions DMI (10 mM; Sigma-Aldrich, Germany) was dissolved in H_2O and Diaz (5 mM; Sigma-Aldrich) in 80% ethanol.

Cell cultures

HEK 293 cells (European Collection of Cell Cultures, UK), WSS-1 cells (ATCC LGC Promochem, Germany) and HEK 293 cells stably expressing the human NMDA receptor NR1A/2A, (NMDA-HEK; Merck, Germany), were cultured in Dulbecco's modified eagle medium (Invitrogen, Germany) supplemented with 10% foetal calf serum (FCS), 1% sodium pyruvate and antibiotics. Cells were reseeded onto fresh Petri dishes twice weekly after treatment with 1% trypsin-EDTA (Invitrogen). Cells were cultured at 37 °C, 5% CO_2 and 95% humidity.

Primary hippocampal neurons were obtained from rat embryos (E20–E21) and were transferred to Ca^{2+}- and Mg^{2+}-free Hank's-buffered salt solution (Invitrogen). Cells were dissociated in 0.66% trypsin/0.1% DNAse following 0.05% DNAse/0.3% ovomucoid incubation. After centrifugation, cells were resuspended in MEM (Invitrogen) and plated on poly-DL ornithine/laminin coated Petri dishes. Cells were cultured in $NaHCO_3$/Hepes-buffered MEM supplemented with 5% FCS and 5% horse serum. Glial mitosis was inhibited by cytosine-β-D-arabinofuranoside.

Electrophysiological recordings

Voltage clamp recordings were made in the whole-cell configuration at a holding potential of −70 mV. Compounds were applied using a fast superfusion device with a stepper motor-driven (Warner Instruments LLC, USA) application pipette, made from modified double-barrelled theta glass. This arrangement allows complete exchange of solutions superfusing all receptors expressed on the cell surface within milliseconds. Currents were recorded using an EPC-9 amplifier (HEKA, Germany). Patch clamp pipettes were pulled from borosilicate glass using a horizontal puller (P-97 Puller; Sutter Instruments, USA), with resistances of 3–6 MΩ when filled with intracellular solution. Intracellular solution for NMDA-HEK: 120 mM CsCl; 10 mM EGTA; 1 mM $MgCl_2$; 0.2 mM $CaCl_2$; 10 mM glucose; 22 mM TEACl; 2 mM ATP; 0.2 mM cAMP; pH 7.35. Corresponding extracellular bath solution: 140 mM NaCl; 3 mM KCl; 10 mM glucose; 10 mM Hepes, 0.2 mM $CaCl_2$; 4.5 mM sucrose; pH 7.35. D-Serine (5 μM) was present in all solutions sufficient to cause 80–85% activation of glycine B receptors. Intracellular solution for $GABA_A$ receptor mediated currents from WSS-1 cells: 140 mM KCl; 11 mM EGTA; 10 mM Hepes-KOH; 2 mM $MgCl_2$; 0.1 mM ATP; pH 7.35. Corresponding extracellular bath solution: 162 mM NaCl; 5.3 mM KCl; 0.67 mM NaH_2PO_4; 0.22 mM KH_2PO_4; 5.6 mM glucose; 15 mM Hepes; 2 mM $CaCl_2$; pH 7.4. Antagonism of NMDA receptor-mediated currents was measured in terms of the magnitude of the steady-state blocked current as percentage of the control current. Five cumulatively increasing concentrations of the respective compound were applied in the continuous presence of agonists and the control current for each substance concentration was calculated by a linear projection from the steady-state current before and after substance application, i.e. for the first concentration control current = 0.85 × current before antagonist plus 0.15 × recovery current. For the second substance concentration, these same currents were multiplied by 0.7 and 0.3 respectively and so on. The potency of the compound was assessed by plotting the mean percentage current magnitude against the antagonist concentration and then a curve was fit using the logistic equation for which the variable parameters IC_{50} and Hill coefficient were free and the range and background values were normally set to 100 and 0, respectively. For analysis of GABA-induced currents in WSS-1 cells only results of stable cells showing at least 50% recovery of responses to GABA following the removal of drugs entered the final analysis. To compensate for this effect the % antagonism at each concentration was based on both the control and the recovery current by assuming a linear time-course for the rundown.

Sucrose density gradient centrifugation

Two confluent Petri dishes of cultured cells were washed in ice-cold PBS before resuspension in 800 μl high-salt Hepes buffer (20 mM Hepes, 5 mM EDTA, 1 M NaCl, pH 7.4) supplemented with protease-inhibitor cocktail. For solubilization 1% Triton X-100 was added directly to the saline buffer as described previously (Nothdurfter et al., 2007). Following homogenization and sonification, the suspension was diluted 1:1 with 80% sucrose solution prepared in high-salt Hepes buffer. The solution was then

placed at the bottom of a centrifuge tube (Beckman Coulter, USA) and overlaid with 1400 μl 35% sucrose and finally with 1000 μl 5% sucrose (both prepared in low-salt Hepes buffer: 20 mM Hepes; 5 mM EDTA; 0.5 M NaCl; pH 7.4). Samples were ultracentrifuged at 40 000 rpm (2 10 000 *g*) in a Beckman SW60 rotor for 4 h at 4 °C. Subsequently, 10 fractions (400 μl each) were taken from the top to the bottom of the gradient.

The experimental protocols for mouse brain tissue fractionation were approved by the Ethical Committee on Animal Care and Use of the Government of Bavaria, Germany. Brains of male C57Bl6 mice aged 28–42 d were put into ice-cold artificial cerebrospinal fluid; sagittal slices of the medial prefrontal cortex (350 μM) were prepared using a microtome (HM 650 V; Microm International, Germany). Tissue of one animal was homogenized/sonified in 1 ml high-salt Hepes buffer supplemented with protease-inhibitor cocktail. The suspension was centrifuged at 1000 *g*, 10 min, 4 °C. The supernatant was again centrifuged at 8000 *g*, 10 min, 4 °C. For solubilization the supernatant of the second centrifugation step was supplemented with 0.4% Triton X-100 and incubated for 30 min on ice. The solution (1850 μl) was then diluted 1:1 with 80% sucrose, overlaid with 3200 μl 35% sucrose and 2300 μl 5% sucrose. After ultracentrifugation in an SW41 rotor at 40 000 rpm (2 50 000 *g*) for 4 h at 4 °C, 13 fractions (710 μl each) were collected.

Cholesterol depletion

Cholesterol depletion using low doses of methyl-β-cyclodextrine (MβCD) to maintain cell viability for electrophysiological recordings was performed as described previously (Nothdurfter et al., 2010). Briefly, cells were incubated with 0.25 or 0.5 mM MβCD for 12 h at 37 °C in serum-free DMEM prior to the electrophysiological recordings.

Western blotting

Equal volumes of sucrose gradient fractions were adjusted 1:5 with Laemmli sample buffer. For the detection of $GABA_A$ receptor subunit γ_2, samples were heated at 70 °C, 10 min; all other samples were denaturated at 95 °C, 5 min. SDS-PAGE was performed on 12% gels. After transfer to a nitrocellulose membrane and blocking (TBS-T/5% milk powder), blots were probed with specific antibodies: transferrin receptor (mouse monoclonal, Zymed, USA, dilution 1:1000); caveolin-1 (mouse monoclonal, BD Biosciences, USA, dilution 1:3000); flotillin-1 (mouse monoclonal, BD Biosciences, dilution 1:1000); $GABA_A$ receptor subunit α_1 (goat polyclonal, Santa Cruz Biotechnologies, USA, dilution 1:500); $GABA_A$ receptor subunit β_2 (rabbit polyclonal, Phosphosolutions, Germany, dilution 1:200); $GABA_A$ receptor subunit γ_2 (Centre of Brain Research of the University of Vienna, Austria, dilution 1:1000); NMDA receptor subunit NR1A (goat polyclonal, Santa Cruz Biotechnologies, dilution 1:300). After incubation with horseradish peroxidase-coupled secondary antibodies, specific antibody binding was visualized by ECL chemiluminescence (Amersham Biosciences, Germany).

Quantification of DMI and Diaz

For the quantification of DMI, 250 μl sucrose gradient fractions, 750 μl H_2O, 0.1 ml internal standard solution and 1 ml 2 M sodium hydrogen carbonate buffer (adjusted to pH 10.5) were mixed and supplemented with 5 ml n-hexane/1.5% isoamyl-alcohol. After centrifugation (4000 *g*, 15 min), the organic layer was transferred to a tube containing 0.25 ml 0.18 M phosphoric acid, mixed and centrifuged at 4000 *g* for 10 min. The organic layer was discarded and an aliquot of the aqueous phase was injected for chromatographic separation. For HPLC analysis, a Beckman Coulter (USA) 166 variable-wavelength UV detector and a Beckman Coulter gradient pump 126 Solvent Module equipped with a Beckman Coulter autoinjector 508 autosampler were used. Separations were made on four coupled Chromolith performance RP-18e 100 × 4.6 mm columns (Merck KGa A). The mobile phases (A, 0.22% orthophosphoric acid adjusted to pH 3.5; B, acetonitrile) were degassed in an ultrasonic bath immediately before use. The column temperature was 30 °C, the flow of the mobile phase was 1.5 ml/min. A mobile phase gradient was used for the chromatographic analysis. DMI was determined by UV absorption 214 nm wavelength. Samples were calibrated using spiked samples at different concentrations. The quantification was performed by calculating the internal standard peak:area ratio of the analyte and a regression model was fitted to the peak:area ratio of the compound to internal standard *vs.* concentration.

Diaz concentrations were measured using liquid chromatography/mass spectrometry/mass spectrometry, which consisted of an Agilent 1100 HPLC system (Agilent technologies, Germany) and an API 4000 triple quadrupole mass spectrometer (Applied Biosystems, Germany) equipped with a turbo ion spray ionization interface in positive MRM mode. Chromatographic separation was performed on a GEMINI C 18, 50 mm × 2.0 mm (Phenomenex, USA) with particle size 5 μM. The mobile phase consisted of methanol-H_2O (85:15, v/v) containing 0.1% formic acid and 10 mM ammonium formate. Isocratic separation was performed with a flow rate of 0.2 ml/min and a run time of 4 min. Column oven temperature was adjusted to 40 °C. Protriptyline was selected as the internal standard. The column effluent was monitored at the following transitions: Diaz *m/z* 285.1→154.0 and the internal standard protriptyline 264.3→155.1. Diaz was extracted with a modified liquid/liquid extraction procedure with acetonitrile.

Lowry protein assay

Protein concentration was determined by a modified method of Lowry et al. (1951).

Cholesterol assay

Cholesterol concentrations were determined colorimetrically with a commercial assay kit (Boehringer, Germany).

Statistical analysis

Differences in electrophysiological parameters were compared using *t* tests for paired samples. As a nominal level of significance, $\alpha = 0.05$ was accepted.

Results

Isolation of lipid rafts

In view of the controversial discussion about lipid raft association of proteins in relation to the use of detergents, we analysed the membrane distribution of the lipid raft marker proteins flotillin-1/caveolin-1 and the transferrin receptor, a bona fide non-raft protein, in the absence and presence of detergent. HEK 293 cells (Fig. 1*a*) and mouse neocortex (Fig. 1*b*) were fractionated by sucrose gradient density centrifugation. In the absence of detergent flotillin-1 and caveolin-1 as well as the transferrin receptor were detected both in low buoyant density (LBD) and in high buoyant density (HBD) fractions of sucrose gradients of HEK 293 cells and mouse neocortex. In contrast, the addition of Triton X-100 shifted the transferrin receptor to the HBD fractions, whereas flotillin-1 and caveolin-1 were retained in the LBD fractions, but lost in the HBD fractions. With regard to the distribution of cholesterol within the cell membrane, cholesterol concentrations were enriched predominantly in the LBD fractions of mouse neocortex (Fig. 1*c*, upper panel). Interestingly, the use of detergent did not affect the cholesterol distribution within membrane factions (Fig. 1*c*, lower panel). Thus, methodological issues such as the use of detergent are crucial for the designation of proteins to be raft-associated or not, while cholesterol distribution in the respective membrane fractions remains unaffected. Consequently, we studied the membrane distribution of ionotropic receptor subunits and psychopharmacological compounds both under detergent-free and detergent-containing conditions in the following experiments.

Effect of lipid raft integrity for NMDA receptor modulation by DMI

The antidepressant DMI reduced NMDA-induced cation currents through human NMDA receptor subunits NR1A/2A in a dose-dependent fashion with an IC_{50} value of $2.7 \pm 0.3\ \mu M$ (Fig. 2*a*, *b*). The control NMDA currents and NMDA currents in the presence of different concentrations of DMI reached steady-state after approximately 5 s, thereby assuring correct current analysis after receptor desensitization has been accomplished.

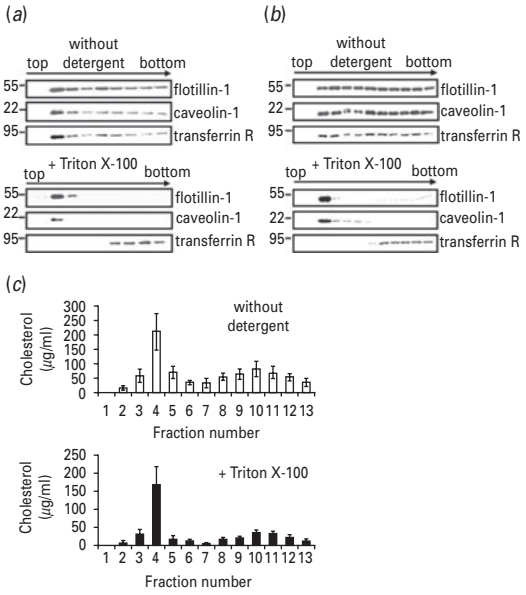

Fig. 1. Effect of detergent on the separation of flotillin-1/caveolin-1 from the transferrin receptor and cholesterol distribution. HEK 293 cells (*a*) and mouse brain neocortex (*b*) were homogenized, sonicated in high-salt buffer and fractionated by sucrose gradient density centrifugation. Fractions were collected and analysed by SDS-PAGE. Replicate gels were immunoblotted with antibodies against flotillin-1, caveolin-1 and the transferrin receptor (transferrin R). One part of HEK 293 cells or mouse neocortical tissue was prepared without detergent, the other part was solubilized with Triton X-100. (*c*) Sucrose gradient fractions of mouse neocortical tissue were assayed for cholesterol concentrations. One part of the tissue was prepared without detergent, the other part was solubilized with Triton X-100. Results represent the means ± S.E.M. of three independent experiments.

To investigate the membrane localization of the NMDA receptor, we fractionated NMDA-HEK cells by sucrose gradient density centrifugation and probed the respective fractions with an antibody against the NMDA receptor subunit NR1A (Fig. 2*c*). When no detergent was used, immunoreactivity was detected both in the low buoyant density fractions (LBD, at the top of the gradient) and in the high buoyant density fractions (HBD, at the bottom of the gradient). The use of Triton X-100 completely shifted the NMDA receptor subunit NR1A to the HBD fractions. To affect lipid raft integrity, we partially depleted cholesterol from cell membranes by means of low-dose MβCD treatment thereby retaining cell viability for subsequent electrophysiological recordings as described previously (Nothdurfter et al., 2010). Pre-treatment of primary hippocampal neurons with 0.1 mM MβCD for 12 h did not alter the inhibitory effect of DMI on NMDA/D-serine-evoked cation currents (Fig. 2*d*, *e*).

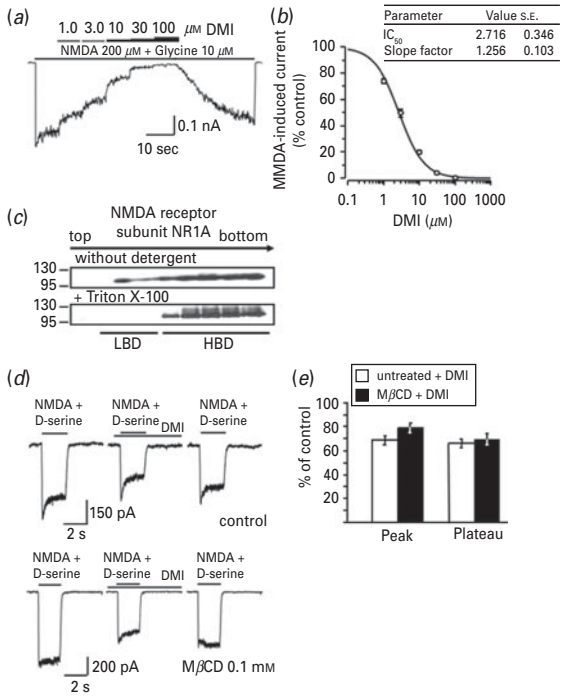

Fig. 2. Inhibitory effect of desipramine (DMI) on NMDA-evoked cation currents and membrane distribution of the NMDA receptor subunit NR1A. (*a*) Cation currents of HEK 293 cells stably expressing NR1/NR2A composed NMDA receptors (NMDA-HEK) were recorded in a whole-cell voltage-clamp configuration. Currents were recorded under a continuous stimulation with 200 μM NMDA in the presence of 10 μM glycine. Cells were exposed to increasing concentrations of DMI (10 to 100 μM). The panel shows representative NR1/2A receptor currents. The upper bar indicates increasing concentrations of DMI; the lower bar indicates the presence of NMDA/glycine. (*b*) Dose–response relationship of DMI against the current amplitude. Results are expressed in % of the control NMDA-induced currents obtained without DMI and represent the means $\pm$ S.E.M. of five independent experiments. (*c*) Membrane fractions of NMDA-HEK cells were prepared by means of sucrose gradient density centrifugation and were analysed by SDS-PAGE. Replicate gels were immunoblotted with a polyclonal antibody against the NMDA receptor subunit NR1. One part of the cells was prepared without detergent, the other part was solubilized with Triton X-100. LBD, low buoyant density fractions; HBD, high buoyant density fractions. (*d*) Cation currents of primary hippocampal neurons were recorded in a whole-cell voltage-clamp configuration. 200 μM NMDA/5 μM D-serine was applied for 2 s in the absence or presence of 3 μM DMI. One portion of cells was pre-treated with 0.1 mM methyl-β-cyclodextrine (MβCD) for 12 h prior to the recordings (lower panel), the other portion of cells remained untreated (control; upper panel). The upper bar indicates the presence of NMDA/D-serine, the lower bar indicates the presence of DMI. One representative recording is shown, respectively. (*e*) Peak amplitude and plateau of untreated cells and after pre-treatment with 0.1 mM MβCD for 12 h of seven independent experiments are shown in the presence of 3 μM DMI in relation to values in the absence of DMI, which are set as 100% (control). Data are shown as means $\pm$ S.E.M. % of control. *t* Tests for paired samples revealed no statistically significant differences between peaks and plateaus of untreated and MβCD pretreated cells.

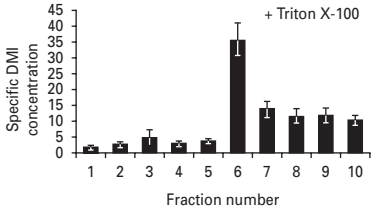

Fig. 3 Accumulation of desipramine (DMI) in membrane fractions of HEK 293 cells in the presence of detergent (Triton X-100). HEK 293 cells were incubated with 10 μM DMI for 30 min at 37 °C. After homogenization and sonification cells were fractionated by sucrose gradient density centrifugation. Fractions were collected and the concentrations of DMI were determined by HPLC. Results are expressed as specific concentration of DMI (ng DMI/mg protein). Data are means $\pm$ S.E.M. of three independent experiments of homogenates solubilized with Triton X-100. Under detergent-free conditions, DMI was preferentially enriched in the low buoyant density fractions (data not shown; Eisensamer et al., 2005).

Membrane distribution of desipramine and diazepam and colocalization with the NMDA and $GABA_A$ receptor

To determine whether the addition of detergent also affects the differential accumulation of psychopharmacological compounds, we quantified the concentrations of DMI in sucrose gradient fractions of HEK 293 cells after incubation with 10 μM DMI. As shown previously (Eisensamer et al., 2005), DMI was enriched in the LBD fractions using a detergent-free preparation procedure. However, the addition of Triton X-100 caused a shift of DMI to the HBD fractions (Fig. 3). Thus, the membrane distribution of both proteins and antidepressive compounds appears to be sensitive to the use of detergent.

Considering the antagonistic effects of DMI at the NMDA receptor we investigated whether the $GABA_A$ receptor is also sensitive to modulation by DMI. Compared to NMDA-induced currents, $GABA_A$ receptor-mediated currents of WSS-1 cells were only slightly inhibited by DMI even at high concentrations, which are far above those achieved under clinical conditions (Glotzbach and Preskorn, 1982; Fig. 4*a*). Following application of 30 μM DMI, chloride currents were reduced only to 73.0 $\pm$ 5.2% of control (charge of currents expressed as the area under the curve in relation to the charge obtained in the absence of DMI, which is set as 100%). With a reduction to 86.6 $\pm$ 9.8%, the peak of receptor currents was even less affected. To investigate whether this rather moderate modulatory potency of DMI at the $GABA_A$ receptor is related to a divergent distribution of the compound and receptor subunits within the cell membrane, we studied the membrane localization of $GABA_A$ receptor subunits in WSS-1 cells

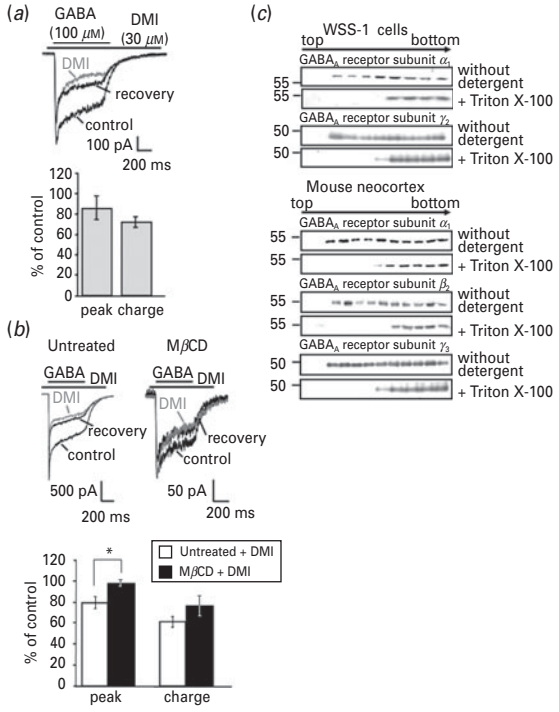

Fig. 4. Effect of desipramine (DMI) on GABA-evoked chloride currents and membrane distribution of $GABA_A$ receptor subunits. (*a*) 30 μM DMI was applied to WSS-1 cells containing recombinant $\alpha_1\gamma_2$ and low levels of endogenous β_3 $GABA_A$ receptor subunits. Chloride currents were recorded in a whole-cell voltage-clamp configuration under conditions of a 500 ms stimulation with 100 μM GABA. The upper panel shows a representative original recording. The upper bar indicates the presence of GABA; the lower bar indicates the presence of DMI. The lower panel shows peak amplitude and charge expressed as the area under the curve (AUC) of the GABA-evoked currents in relation to values obtained in the absence of DMI, which is set as 100% (% of control). Data are presented as the means ± S.E.M. of ten independent experiments. For calculation of the final DMI effect, values from control and recovery traces were included into the analysis. (*b*) 30 μM DMI was applied to WSS-1 cells in serum-free medium (untreated) and after cholesterol depletion induced by 0.5 mM methyl-β-cyclodextrine (MβCD). Chloride currents were recorded in a whole-cell voltage-clamp configuration under conditions of a 500 ms stimulation with 100 μM GABA. The upper panel shows representative original recordings. The upper bar indicates the presence of GABA; the lower bar indicates the presence of DMI. The lower panel shows peak amplitude and charge expressed as the AUC of the GABA-evoked currents in relation to values obtained in the absence of DMI, which is set as 100% (% of control). Data are presented as the means ± S.E.M. of five independent experiments, respectively. For calculation of the final DMI effect, values from control and recovery traces were included into the analysis. *T* tests for paired samples revealed a statistically significant difference between peaks of untreated and MβCD pre-treated cells; * $p < 0.05$. (*c*) WSS-1 cells and mouse neocortical tissue were homogenized, sonicated and fractionated by sucrose gradient density centrifugation either in the presence or absence of detergent. Fractions of the gradient were collected and analysed by SDS-PAGE. Replicate gels were immunoblotted with antibodies against the $GABA_A$ receptor subunits α_1, β_2 (for mouse neocortex) and γ_2. The expression of the β_3 subunit in WSS-1 cells was below the limit of detection by Western blotting.

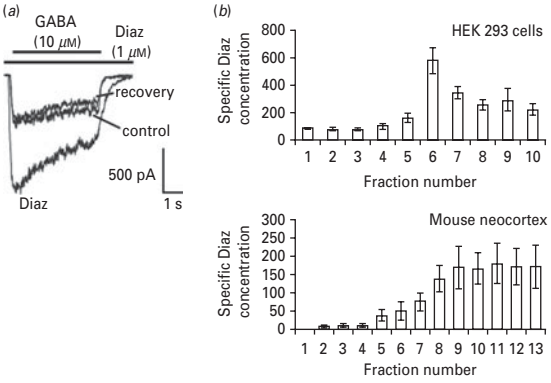

Fig. 5. Potentiation of GABA-evoked chloride currents by diazepam (Diaz) and membrane distribution of Diaz. (*a*) Diaz (1 μM) was applied to WSS-1 cells containing $\alpha_1\beta_3\gamma_2$ $GABA_A$ receptor subunits. Chloride currents were recorded in a whole-cell voltage-clamp configuration under conditions of 5 s stimulation with 10 μM GABA. A representative original recording is shown. The upper bar indicates the presence of GABA; the lower bar indicates the presence of Diaz. (*b*) HEK 293 cells (upper panel) or mouse brain neocortex (lower panel) were incubated with 1 μM Diaz for 30 min at 37 °C. After homogenization and sonification cells and tissue were fractionated by sucrose gradient density centrifugation in the absence of detergent. Fractions were collected and analysed for the concentrations of Diaz by mass spectrometry. Results are expressed as specific concentration of Diaz (ng Diaz/mg protein). Data are expressed as means ± S.E.M. of three independent experiments.

(α_1 and γ_2) and mouse neocortex (α_1, β_2 and γ_2; Fig. 4*c*). Similarly to the NMDA receptor, all $GABA_A$ receptor subunits were detected both in LBD and HBD fractions of cells and tissue using a detergent-free protocol, but only in the HBD fractions when using Triton X-100. Thus, the membrane distribution of $GABA_A$ receptor subunits does not explain the considerably weaker effect of DMI at this ligand-gated ion channel. Interestingly, the inhibitory potency of DMI on $GABA_A$ receptor-mediated currents appeared to be partially reversed under cholesterol-depleting conditions (charge: 61.5 ± 5.0% untreated *vs.* 75.5 ± 10.7% MβCD pre-treated; peak: 79.2 ± 5.6% untreated *vs.* 97.5 ± 3.4% MβCD pre-treated; Fig. 4*b*).

Benzodiazepines are potent positive allosteric modulators of $GABA_A$ receptors. We therefore investigated the modulatory properties of Diaz on $GABA_A$ receptor function in relation to the membrane distribution of $GABA_A$ receptor subunits and that of Diaz. As shown previously (Davies et al., 2000), 1 μM Diaz markedly potentiated GABA-evoked chloride currents of WSS-1 cells (235.7 ± 15.2%; charge of the currents expressed as the area under the curve in relation to the charge obtained in the absence of Diaz, which is set as 100%; data represent

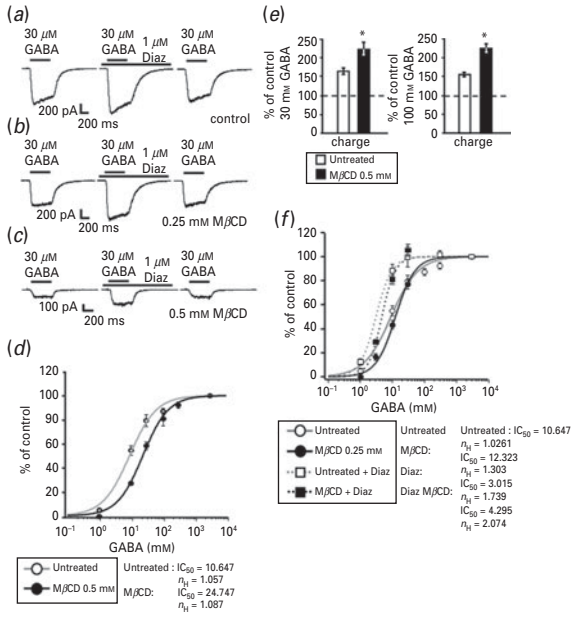

Fig. 6 Effect of methyl-β-cyclodextrine (MβCD) induced cholesterol depletion of WSS-1 cells on GABA-evoked chloride currents and their modulation by diazepam (Diaz). (*a*) Potentiating effect of Diaz at the GABA$_A$ receptor of WSS-1 cells. Chloride currents were recorded in a whole-cell voltage-clamp configuration. 30 μM GABA were applied for 500 ms in the absence or presence of 1 μM Diaz. The upper bars indicate the presence of GABA, the lower bar indicates the presence of Diaz. Representative recordings before and after application of Diaz and subsequent washout are shown. Potentiating effect of Diaz at the GABA$_A$ receptor of WSS-1 cells after cholesterol depletion induced by 0.25 mM MβCD (*b*) or 0.5 mM MβCD (*c*). Chloride currents were recorded in a whole-cell voltage-clamp configuration. GABA (30 μM) were applied for 500 ms in the absence or presence of 1 μM Diaz. The upper bars indicate the presence of GABA, the lower bar indicates the presence of Diaz. Representative recordings before and after application of Diaz and subsequent washout are shown. Cells were treated with 0.25/0.5 mM MβCD for 12 h prior to the recordings. (*d*) Dose–response relationship of the GABA-evoked current charge through the GABA$_A$ receptor of untreated WSS-1 cells and of WSS-1 cells pre-treated with 0.5 mM MβCD. Results are normalized to the maximum receptor current induced by 3 mM GABA and presented as means $\pm$ S.E.M. of seven independent experiments. (*e*) Charges of untreated cells and after pre-treatment with 0.5 mM MβCD for 12 h evoked by 30 μM GABA (left panel) or 100 μM GABA (right panel) in the presence of 1 μM Diaz of five independent experiments in relation to values in the absence of Diaz, which are set as 100% (control). Data are shown as means $\pm$ S.E.M. % of control (currents evoked with 30 or 100 μM GABA). Statistically significant differences between charges of untreated and MβCD pre-treated cells (*t* test for paired samples, * $p < 0.05$). (*f*) Dose–response relationship of the GABA-evoked current charge through the GABA$_A$ receptor of untreated WSS-1 cells and of WSS-1 cells pre-treated with 0.25 mM MβCD. Results are normalized to the maximum receptor current induced by 3 mM GABA and presented as means $\pm$ S.E.M. of five independent experiments. Also presented are means $\pm$ S.E.M. of normalized charges of untreated WSS-1 cells treated with 1 μM Diaz of four independent experiments and means $\pm$ S.E.M. of normalized charges of WSS-1 cells pre-treated with 0.25 mM MβCD treated with 1 μM Diaz of four independent experiments. n_H, Hill coefficient.

the means $\pm$ S.E.M. of five independent experiments; Fig. 5*a*). This potentiating effect was antagonised by 10 μM flumazenil (data not shown). The distribution of Diaz within the cell membrane was determined in sucrose gradient fractions of HEK 293 cells and mouse neocortex after incubation with 1 μM Diaz (Fig. 5*b*). In contrast to DMI, which was enriched in the LBD fractions, Diaz preferentially accumulated in the HBD non-raft fractions already under detergent-free conditions. This distribution pattern was not altered when Triton X-100 was used for preparation of lipid rafts (data not shown). Thus, both ligand-gated ion channel subunits and psychopharmacological compounds show different distribution patterns within the cell membrane with regard to lipid raft association.

Effect of lipid raft integrity for GABA$_A$ receptor modulation by Diaz

Impairment of lipid raft integrity by pre-treatment of WSS-1 cells with MβCD for 12 h dose-dependently diminished GABA-evoked chloride currents (Fig. 6*a–c*). The shift of the GABA dose–response curve to the right after MβCD treatment (Fig. 6*d*) indicates reduced agonist effectiveness when receptors are not integrated in lipid rafts. When receptors were activated at submaximal GABA concentrations (Fig. 6*e*) the GABA enhancing effect of Diaz i.e. increase in GABA potency was even more pronounced under MβCD pre-treatment conditions. However, the maximal Diaz-induced potentiation of receptor currents did not change (Fig. 6*f*), i.e. maximal currents observed with saturating concentrations of GABA were the same both in the presence and absence of Diaz.

Because cholesterol depletion decreased membrane stability and deteriorated patch-clamp recording conditions the generation of a concentration–response curve in the presence of Diaz was not achievable with 0.5 mM MβCD. However, leak current and membrane resistance of HEK cells after treatment with 0.5 mM MβCD were comparable to those cells that were untreated. Pre-treatment with 0.25 mM MβCD reduced membrane cholesterol content to 82.10% of control (data not shown). Consequently, this concentration did not result in a sufficient shift to the right of the GABA concentration–response curve as observed at 0.5 mM MβCD. These results indicate that substantial amounts of GABA$_A$ receptors were still incorporated into lipid rafts.

Discussion

In the present study we investigated the membrane distribution of NMDA and GABA$_A$ receptor subunits in

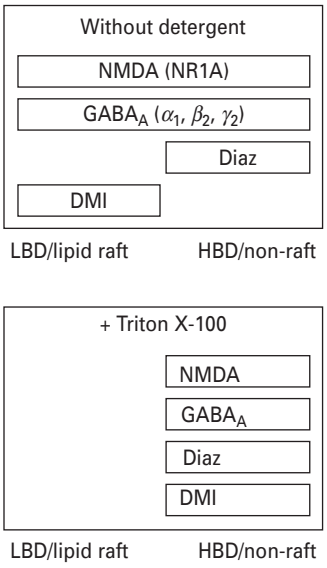

Fig. 7. Schematic diagram showing the distribution of receptors and compounds in lipid raft and non-raft membrane fractions of sucrose gradients. Diaz, diazepam; DMI, desipramine; LBD, low buoyant density fractions; HBD, high buoyant density fractions.

relation to their allosteric modulation by DMI and Diaz. The assignment of receptor subunits and drugs to specific membrane fractions turned out to be strongly dependent on the preparation procedure. A partial colocalization of receptor subunits and the compounds within the cell membrane was found under detergent-free conditions and a complete overlap in non-raft fractions when using detergent (Fig. 7). Impairment of lipid raft integrity by cholesterol depletion did not substantially alter the modulatory potency of DMI at the NMDA and GABA$_A$ receptor. However, impairment of lipid raft integrity affected the positive allosteric modulation of the GABA$_A$ receptor by benzodiazepines.

Preparation of lipid rafts heavily relies on the purification method employed. Commonly, lipid rafts are considered as membrane fractions that are resistant to non-ionic detergents such as Triton X-100 (Brown and Rose, 1992). In fact, we found that the use of detergent allowed proper separation of the lipid raft marker proteins caveolin-1 and flotillin-1 from the transferrin receptor, which is widely considered as a non-raft protein (Nothdurfter et al., 2007). This is in line with previous findings reporting a dose-dependent effect of Triton X-100 on the separation of raft from non-raft proteins (Brady et al., 2004). On the other hand, the use of detergent-free protocols has been suggested to more closely reflect the physiological situation (Schnitzer et al., 1995a, b; Smart et al., 1995; Song et al., 1996; Luria et al., 2002; Eisensamer et al., 2005; Persaud-Sawin et al., 2009). Accordingly, different compositions and properties of lipid rafts have been reported depending on the extraction method used (Foster et al., 2003; Kim et al., 2004; Sprenger and Horrevoets, 2007; Garner et al., 2008; Pike, 2009). Consequently, we studied the membrane distribution of ligand-gated ion channels and psychopharmacological compounds under both detergent-free and detergent-containing conditions in the present study. The detergent-free protocol revealed a much more differential distribution pattern of ionotropic receptor subunits and compounds investigated, although the separation of prototypical markers of raft and non-raft proteins appeared more challenging.

Concerning the NMDA receptor, the NR1A subunit has been located in non-raft membrane fractions of rat forebrain when using an Optiprep gradient without detergent solubilization (Wu et al., 1997). In a study by Hering et al. (2003), NR1 was found both in raft and in non-raft fractions under detergent-containing conditions. A non raft-association has been reported for the NR1, NR2A and NR2B subunits using Triton X-100 as a detergent (Suzuki et al., 2001). Besshoh et al. (2007) found lipid raft association of the NR2A subunit under detergent-containing conditions, whereas the NR2B subunit in rat brain tissue shifted from post-synaptic densities to lipid rafts with increasing age. A study by Ponce et al. (2008) suggested an important role of lipid raft integrity for NMDA receptor function, showing that the reduction of cholesterol levels by simvastatin might protect from NMDA-induced neuronal damage by reducing the association of the NR1 subunit with lipid rafts. In our study, impairment of lipid raft integrity by cholesterol depletion did not affect the modulatory potency of DMI at the NMDA receptor, which suggests that the membrane localization of this receptor and compound plays a minor role for its modulation by this antidepressant. In some contrast to the NMDA receptor, lipid raft impairment partially reversed the antagonistic effect of DMI at the GABA$_A$ receptor, although this effect appeared only marginally. Detergent-free lipid raft preparation yielded a clear distribution of both DMI and partially GABA$_A$ receptor subunits in the raft fractions. Thus, cholesterol depletion might interfere with the pharmacological effects of DMI on GABA$_A$ receptors by e.g. impairing ligand × receptor interaction, thereby weakening the antagonistic potency.

With regard to lipid raft association of GABA$_A$ receptors, an almost exclusive lipid raft association has been claimed for the α_1 subunit of rat cerebellar granule cells after purification with the detergent Brij 98 (Dalskov et al., 2005). Following multiple solubilization steps with Triton X-100 of rat forebrain tissue, distinct GABA$_A$ receptor subunit combinations have been attributed to different cell membrane compartments (Li et al., 2007). The α and β subunits in the absence of γ subunits, which might represent extra-synaptic receptors, have been detected in detergent-resistant membranes/lipid rafts. In contrast, synaptic assemblies containing α and β subunits together with the γ_2 subunit showed only negligible lipid raft association.

In our study, the use of the detergent Triton X-100 shifted NMDA and $GABA_A$ receptor subunits to the HBD fractions of sucrose gradients. However, when using a detergent-free protocol, a much more differential distribution pattern of ionotropic receptors within the cell membrane could be observed. NMDA receptor (NR1A subunit) and $GABA_A$ receptor subunits (α_1, β_2, γ_2) were distributed both over the LBD and the HBD fractions of the sucrose gradient. In contrast, the 5-HT_3 receptor was located predominantly in the lipid raft-associated LBD fractions (Eisensamer et al., 2005; Nothdurfter et al., 2010). Presumably, physiological and pharmacological processes are more reliably reflected using detergent-free protocols.

Currently, only few data are available concerning the distribution of psychopharmacological drugs within membrane fractions. The tricyclic antidepressant DMI, which modulates the 5-HT_3 receptor in a non-competitive manner (Eisensamer et al., 2003), was predominantly accumulated in raft-like domains and colocalized with the 5-HT_3 receptor protein under detergent-free conditions as shown previously for various other antidepressants and antipsychotics (Eisensamer et al., 2005). However, the addition of Triton-X-100 during preparation completely shifted DMI to the HBD fractions, but had no effect on the cholesterol distribution within the cell membrane. These results are in contrast to the benzodiazepine Diaz, which was enriched in the HBD fractions already under detergent-free conditions. Thus, in spite of their common lipophilic properties, various psychopharmacological compounds display a differential association with lipid rafts, which might contribute to their distinct psychopharmacological profile.

It has been shown previously that the tricyclic antidepressant DMI acts as a functional antagonist at the NMDA receptor (Sernagor et al., 1989; Watanabe et al., 1993; Szasz et al., 2007). Our experiments performed with NMDA receptors expressed in HEK cells confirm these results. Furthermore, currents showed a nearly complete recovery to the control steady-state level after removal of the antagonist. This observation and the fact that the original cytosolic content is mainly dominated by the intracellular pipette solution with no protein left, renders a DMI-mediated mechanism via receptor internalisation unlikely and rather speaks in favour of a direct antagonism at the receptor. Although the concentrations required for these modulatory effects are in the low micromolar range, they are nevertheless of clinical relevance in view of a high brain: plasma ratio of tricyclic antidepressants (Glotzbach and Preskorn, 1982). On the other hand, DMI delivered at rather high concentrations only slightly affected GABA-evoked chloride currents, thereby indicating that the effect of DMI on $GABA_A$ receptors appears to be less potent as compared to NMDA receptors and is not of clinical relevance. Thus, the colocalization of DMI with subunits of ionotropic receptors seems not to be sufficient for a potent allosteric receptor modulation in general.

The benzodiazepine Diaz markedly potentiated GABA-evoked chloride currents, which is in line with previous studies (Davies et al., 2000). Diaz was colocalized with $GABA_A$ receptor subunits in the HBD fractions already under detergent-free conditions, which supports the hypothesis that synaptic $GABA_A$ receptors, which are sensitive to benzodiazepines, are located predominantly within non-raft fractions (Li et al., 2007). To investigate the role of the membrane localization of the $GABA_A$ receptor for its modulation by benzodiazepines we impaired lipid raft integrity by MβCD-induced cholesterol depletion. MβCD treatment diminished $GABA_A$ receptors currents *per se*, similarly to the results previously found for the 5-HT_3 receptor (Nothdurfter et al., 2010). The potentiating effect of Diaz appeared to be enhanced at lower GABA concentrations under cholesterol-depleting conditions. However, due to technical limitations related to cholesterol depletion, we could not perform Schild plot analysis which would have provided definite clarity about the effects of benzodiazepines at the $GABA_A$ receptor under conditions of cholesterol depletion. Nevertheless, our results suggest that, at submaximal GABA concentrations, benzodiazepines show an increased effectiveness at $GABA_A$ receptors after cholesterol depletion. Together with the preferential accumulation of Diaz in non-raft fractions, these results argue for the hypothesis that the interaction of benzodiazepines with the $GABA_A$ receptor likely occurs outside lipid rafts.

Acknowledgements

HEK 293 cells stably expressing the NMDA receptor NR1A/2A were a generous gift from Merck, Darmstadt, Germany. The $GABA_A$ receptor subunit γ_2 antibody was a generous gift from Werner Sieghart from the Centre of Brain Research of the University of Vienna, Austria. The authors thank Christian Namendorf and Annette Schubert for performing the quantification of psychopharmacological compounds, Peter Altrichter (Centre of Brain Research of the University of Vienna) for assistance with the Western blots of the $GABA_A$ receptor subunit γ2 and Thomas Kirmeier and Julia S. Kessler for valuable discussion.

Statement of Interest

None.

References

Allen JA, Halverson-Tamboli RA, Rasenick MM (2007) Lipid raft microdomains and neurotransmitter signalling. Nat Rev Neurosci 8:128–140.

Besshoh S, Chen S, Brown IR, Gurd JW (2007) Developmental changes in the association of NMDA receptors with lipid rafts. J Neurosci Res 85:1876–1883.

Brady JD, Rich TC, Le X, Stafford K, Fowler CJ, Lynch L, Karpen JW, Brown RL, Martens JR (2004) Functional role of

lipid raft microdomains in cyclic nucleotide-gated channel activation. Mol Pharmacol 65:503–511.
Brown DA, Rose JK (1992) Sorting of GPI-anchored proteins to glycolipid-enriched membrane subdomains during transport to the apical cell surface. Cell 68:533–544.
Dalskov SM, Immerdal L, Niels-Christiansen LL, Hansen GH, Schousboe A, Danielsen EM (2005) Lipid raft localization of GABA A receptor and Na+, K+-ATPase in discrete microdomain clusters in rat cerebellar granule cells. Neurochem Int 46:489–499.
Davies PA, Hoffmann EB, Carlisle HJ, Tyndale RF, Hales TG (2000) The influence of an endogenous beta3 subunit on recombinant GABA(A) receptor assembly and pharmacology in WSS-1 cells and transiently transfected HEK293 cells. Neuropharmacology 39: 611–620.
Donati RJ, Dwivedi Y, Roberts RC, Conley RR, Pandey GN, Rasenick MM (2008) Postmortem brain tissue of depressed suicides reveals increased Gs alpha localization in lipid raft domains where it is less likely to activate adenylyl cyclase. J Neurosci 28:3042–3050.
Donati RJ, Rasenick MM (2005) Chronic antidepressant treatment prevents accumulation of gsalpha in cholesterol-rich, cytoskeletal-associated, plasma membrane domains (lipid rafts). Neuropsychopharmacology 30:1238–1245.
Eisensamer B, Rammes G, Gimpl G, Shapa M, Ferrari U, Hapfelmeier G, Bondy B, Parsons C, Gilling K, Zieglgänsberger W (2003) Antidepressants are functional antagonists at the serotonin type 3 (5-HT3) receptor. Mol Psychiatry 8:994–1007.
Eisensamer B, Uhr M, Meyr S, Gimpl G, Deiml T, Rammes G, Lambert JJ, Zieglgänsberger W, Holsboer F, Rupprecht R (2005) Antidepressants and antipsychotic drugs colocalize with 5-HT3 receptors in raft-like domains. J Neurosci 25:10198–10206.
Foster LJ, De Hoog CL, Mann M (2003) Unbiased quantitative proteomics of lipid rafts reveals high specificity for signaling factors. Proc Natl Acad Sci USA 100:5813–5818.
Garner AE, Smith DA, Hooper NM (2008) Visualization of detergent solubilization of membranes: implications for the isolation of rafts. Biophys J 94:1326–1340.
Glotzbach RK, Preskorn SH (1982) Brain concentrations of tricyclic antidepressants: single-dose kinetics and relationship to plasma concentrations in chronically dosed rats. Psychopharmacology (Berl) 78:25–27.
Guirland C, Suzuki S, Kojima M, Lu B, Zheng JQ (2004) Lipid rafts mediate chemotropic guidance of nerve growth cones. Neuron 42:51–62.
Hering H, Lin CC, Sheng M (2003) Lipid rafts in the maintenance of synapses, dendritic spines, and surface AMPA receptor stability. J Neurosci 23:3262–3271.
Kim KB, Kim SI, Choo HJ, Kim JH, Ko YG (2004) Two-dimensional electrophoretic analysis reveals that lipid rafts are intact at physiological temperature. Proteomics 4:3527–3535.
Kusumi A, Suzuki K (2005) Toward understanding the dynamics of membrane-raft-based molecular interactions. Biochim Biophys Acta 1746:234–251.
Li X, Serwanski DR, Miralles CP, Bahr BA, De Blas AL (2007) Two pools of Triton X-100-insoluble GABA(A) receptors are present in the brain, one associated to lipid rafts and another one to the post-synaptic GABAergic complex. J Neurochem 102:1329–1345.
Lowry OH, Rosebrough NJ, Farr AL, Randall RJ (1951) Protein measurement with the Folin phenol reagent. J Biol Chem 193:265–275.
Luria A, Vegelyte-Avery V, Stith B, Tsvetkova NM, Wolkers WF, Crowe JH, Tablin F, Nuccitelli R (2002) Detergent-free domain isolated from Xenopus egg plasma membrane with properties similar to those of detergent-resistant membranes. Biochemistry 41:13189–13197.
Nothdurfter C, Rammes G, Rein T, Rupprecht R (2007) Pitfalls in isolating lipid rafts. Nat Rev Neurosci 8:567.
Nothdurfter C, Tanasic S, Di Benedetto B, Rammes G, Wagner EM, Kirmeier T, Ganal V, Kessler JS, Rein T, Hoslboer F, Rupprecht R (2010) Impact of lipid raft integrity on 5-HT3 receptor function and its modulation by antidepressants. Neuropsychopharmacology 35:1510–1519.
Patel HH, Murray F, Insel PA (2008) Caveolae as organizers of pharmacologically relevant signal transduction molecules. Ann Rev Pharmacol Toxicol 48:359–391.
Persaud-Sawin DA, Lightcap S, Harry GJ (2009) Isolation of rafts from mouse brain tissue by a detergent-free method. J Lipid Res 50:759–767.
Pike LJ (2004) Lipid rafts: heterogeneity on the high seas. Biochem J 378:281–292.
Pike LJ (2009) The challenge of lipid rafts. J Lipid Res 50(Suppl.):S323–S328.
Ponce J, de la Ossa NP, Hurtado O, Millan M, Arenillas JF, Davalos A, Gasull T (2008) Simvastatin reduces the association of NMDA receptors to lipid rafts: a cholesterol-mediated effect in neuroprotection. Stroke 39:1269–1275.
Rammes G, Eisensamer B, Ferrari U, Shapa M, Gimpl G, Gilling K, Parsons C, Riering K, Hapfelmeier G, Bondy B, Zieglgänsberger W, Holsboer F, Rupprecht R (2004) Antipsychotic drugs antagonize human serotonin type 3 receptor currents in a noncompetitive manner. Mol Psychiatry 9:846–858, 818.
Schnitzer JE, McIntosh DP, Dvorak AM, Liu J, Oh P (1995a) Separation of caveolae from associated microdomains of GPI-anchored proteins. Science 269:1435–1439.
Schnitzer JE, Oh P, Jacobson BS, Dvorak AM (1995b) Caveolae from luminal plasmalemma of rat lung endothelium: microdomains enriched in caveolin, Ca(2+)-ATPase, and inositol trisphosphate receptor. Proc Natl Acad Sci USA 92:1759–1763.
Sernagor E, Kuhn D, Vyklicky Jr. L, Mayer ML (1989) Open channel block of NMDA receptor responses evoked by tricyclic antidepressants. Neuron 2:1221–1227.
Smart EJ, Ying YS, Mineo C, Anderson RG (1995) A detergent-free method for purifying caveolae membrane from tissue culture cells. Proc Natl Acad Sci USA 92:10104–10108.
Song KS, Li S, Okamoto T, Quilliam LA, Sargiacomo M, Lisanti MP (1996) Co-purification and direct interaction of Ras with caveolin, an integral membrane protein of caveolae microdomains. Detergent-free purification of caveolae microdomains. J Biol Chem 271:9690–9697.
Sprenger RR, Horrevoets AJ (2007) The ins and outs of lipid domain proteomics. Proteomics 7:2895–2903.
Suzuki T, Ito J, Takagi H, Saitoh F, Nawa H, Shimizu H (2001) Biochemical evidence for localization of AMPA-type

glutamate receptor subunits in the dendritic raft. Brain Res Mol Brain Res 89:20–28.

Szasz BK, Mike A, Karoly R, Gerevich Z, Illes P, Vizi ES, Kiss JP (2007) Direct inhibitory effect of fluoxetine on *N*-methyl-D-aspartate receptors in the central nervous system. Biol Psychiatry 62:1303–1309.

Tsui-Pierchala BA, Encinas M, Milbrandt J, Johnson Jr. EM (2002) Lipid rafts in neuronal signaling and function. Trends Neurosci 25:412–417.

Watanabe Y, Saito H, Abe K (1993) Tricyclic antidepressants block NMDA receptor-mediated synaptic responses and induction of long-term potentiation in rat hippocampal slices. Neuropharmacology 32:479–486.

Wu C, Butz S, Ying Y, Anderson RG (1997) Tyrosine kinase receptors concentrated in caveolae-like domains from neuronal plasma membrane. J Biol Chem 272:3554–3559.